

Optimization of Ethanol Reforming with micro-channels in Plate type reformer configuration

Somasree Roychowdhury, P K Vivekanand, Sarit Kumar Das
and Thirumalachari Sundararajan*

Department of Mechanical Engineering, Indian Institute of Technology Madras, Chennai, Tamil Nadu, India - 600036

[Received date; Accepted date] – to be inserted later

Abstract

The study of steam reforming of ethanol in micro-channels in a plate-type reformer has been carried out to understand the fluid mechanics, heat transfer and kinetics of ethanol conversion to hydrogen for fuel-cell applications. Heat exchange between alternate channels of combustion flue gas and steam-ethanol mixture has been considered, involving co-flow or counter-flow configurations. Combustion reactions are observed to be completed close to the entry. This results in higher rates of conversion for the co-flow configuration, owing to higher heat transfer rates at the entry. It is shown that end effects are felt only in the outer-most channels and hence a symmetric reformer channel analysis is adequate to predict the performance of a multi-channel reformer system. In the axial direction, the flow, temperature and concentration fields attain fully developed profile form at a short distance from the inlet. At larger axial distances, the velocity profile undergoes mild variations due to changes in the gas density. The temperature and concentration profiles become flat, indicating the weak role played by diffusive transport on the reforming process. In fact, dimensionless temperature and concentration profiles are identical within the reformer channel, leading to the conclusion that the reforming reaction is primarily controlled by conjugate heat transfer between the flue gas and reformer channel systems. The heat transfer area and convective film resistances in the flue gas and reformer channels play a major role in influencing the conversion efficiency. Thus a reformer with relatively shorter length, larger width and larger channel gap gives rise to higher ethanol conversion efficiency, in parallel flow heat exchange configuration.

1. INTRODUCTION

Hydrogen based fuel cells have received considerable attention in recent times, because they are environment friendly and offer higher energy conversion efficiencies. However, deployment of hydrogen entails inherent disadvantages such as – high explosion risk and cumbersome storage. Hence, production of hydrogen *in situ* before its usage in fuel cell is an interesting concept. There are two main methods to produce hydrogen namely, water electrolysis and reforming a hydrocarbon, alcohol or any other organic compound. The reforming method involves much lower energy consumption as compared to electrolysis.

In the present study, attention is being focused on the production of hydrogen from ethanol, in a 'Reformer'. A reformer is like a heat exchanger in construction, with the additional feature of a catalyst bed or coating, to facilitate the endothermic reforming reactions. Among various configurations such as shell & tube, plate-type and diaphragm-based systems, the plate-type micro-channel reformers appear to be attractive options from compactness point of view.

*Corresponding author: E-mail address: tsundar@iitm.ac.in

Due to the easy production of ethanol from biomass sources, steam reforming of ethanol (SRE) has been widely investigated. The reforming of ethanol on a flat plate catalytic wall reactor with Rh and Rh–Ce catalysts was investigated by Wanat et al. [1], in which the ethanol conversion rate was reported to be more than 99%, at a steam-carbon ratio of 3:1. Sahoo et al. [2] studied the performance of Co/Al₂O₃ catalyst on SRE in a fixed bed stainless steel reactor. They have reported the effects of temperature, contact time, steam to ethanol molar ratio, etc. on ethanol conversion. The influence of increase in water to ethanol ratio on the hydrogen yield and ethanol conversion was analyzed by Leclerc et al. [3]. Studies have been performed on the kinetics of SRE over various catalysts using the power law model, which shows that the ethanol consumption rate is first order with respect to ethanol concentration and is nearly independent of steam concentration [4 - 6]. Aboudheir et al. [7] found the assumptions of plug flow and isothermal behavior in the radial direction as justifiable for SRE in a packed bed tubular reactor over Ni/Al₂O₃ catalyst. However, the axial dispersion terms in both the mass and energy balance equations could not be neglected. A comparative study of the performance of a micro-channel reactor with that of a packed bed reactor was done by Peela et al. [8], using 2% Rh/ 20% CeO₂/ Al₂O₃ catalyst at identical operating conditions. Although the activity of the catalyst was found to be similar in both the reactors, the micro-channel reactor showed higher selectivity for the desired products. Numerical studies on the steam reforming of methanol, ethanol and propane were performed by Karakaya and Avci [9]. The influence of geometry with the presence of microbaffles within the channels, on heat transfer to the reforming zone and the resulting hydrogen yield was also discussed by them. Several investigators [10 - 14] have reported results from different types of micro-structured reactors and ceramic micro-components.

Although a significant amount of research has been carried out on the kinetics of SRE with various catalysts, there is very little work in the literature regarding the configurational design aspects that significantly influence the efficiency of SRE in micro-channels. Hence, the objective of this study is to understand the transport phenomena and the geometrical aspects involved (in micro-scale) that dictate the behavior of fluid flow, conjugate heat transfer and chemical reactions during the steam reforming of ethanol. The effects of catalyst selectivity are not brought in here explicitly for the sake of simplicity. Choices of configurational parameters that lead to optimal conversion from ethanol to hydrogen are addressed in detail.

2. MATHEMATICAL MODELING

2.1 Problem geometry

Reforming being an endothermic process, heat needs to be supplied to the reforming mixture. In the present study, the heat required for the reforming reaction is also assumed to be produced by a combustion reaction between ethanol and air. Although it is possible to produce this heat simultaneously with reforming in an Auto-thermal reformer, for the sake of better control, separate channels have been considered for the combustion and reforming processes, with effective heat exchange between them. The flow configuration and channel dimensions such as channel length, cross-sectional area and plate thickness, play an important role with respect to the conjugate heat transfer between the combustion and reforming processes occurring in neighboring channels.

A plate-type reformer has been considered and for the sake of simplicity, the problem geometry has been approximated as a two-dimensional computational domain. The length, depth and channel gap have been selected as 100mm, 50mm and 2mm respectively for the reference case, based on the literature available [15 - 18] on ethanol reformers. Other values of these geometric parameters have been considered as variants of the reference case.

In general, the reformer system contains many channels as shown in Fig. 1. Initially special cases such as a two-channel system, three-channel system, and five-channel system were studied to provide some useful insights. In order to comprehend the physics involved in an actual system which has multiple channels, an eleven-channel system and a simplified symmetric channel system (half combustor + full reformer + half combustor, as shown in Fig. 1) have also been considered. The symmetric channel system model greatly reduces the computational effort required for simulating the

performance of a multi-channel reformer configuration, with large number of channels. The wall separating each channel has been assumed to have a thickness of 2mm and the material of the wall is taken to be stainless steel. The computational model geometry was created using the commercial pre-processing software Gambit 2.4.

For co-flow in the two-channel or three-channel system, the directions of flow for both the flue gas and reforming mixture were taken in the positive y-direction. For counter-flow systems on the other hand, only the reforming gas flow alone was taken in the positive y-direction with the flue gas from ethanol combustion orienting in the negative y-direction. Effects of gravity were neglected for the small dimensions involved in this problem. Figure 1 shows the flow configuration for a multi-channel co-flow system.

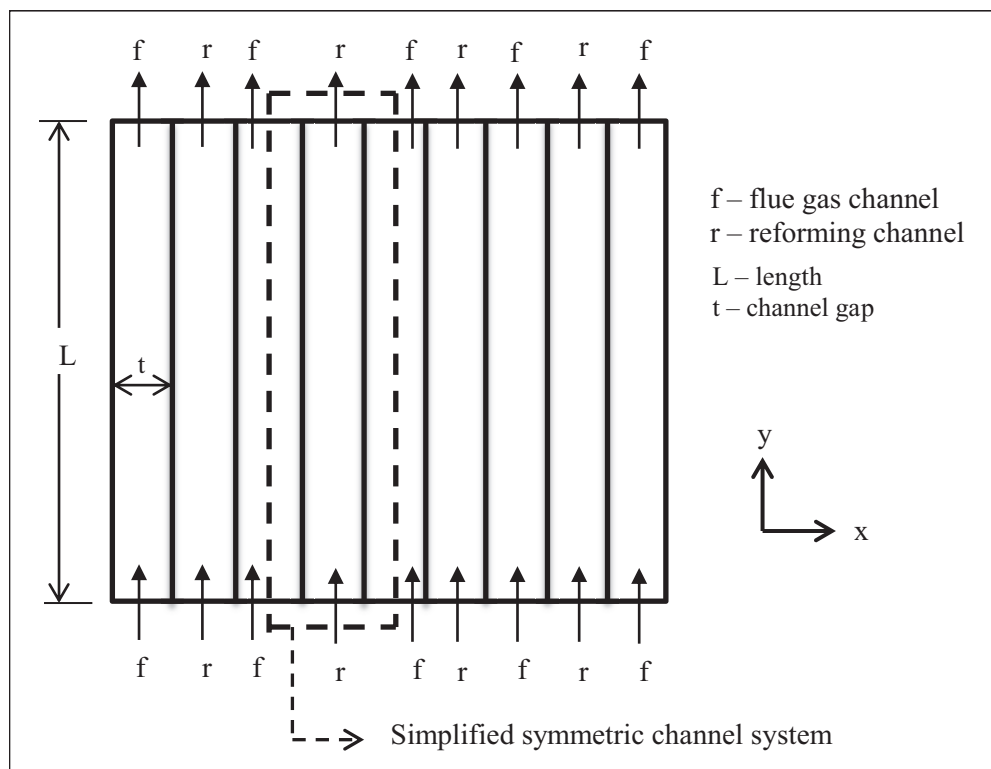


Figure 1. 2-D model of a typical integrated combustor - reformer system

2.2 Governing equations and boundary conditions

2.2.1 Inputs to the model

In the conjugate heat transfer studies, a few initial simulations were performed with aluminium as wall material, which was later changed to stainless steel (as the reformer plates are generally made up of stainless steel). Due to the small pressure drop, the system pressure was essentially taken as atmospheric, with minor variation in pressure due to the flow process. Studies were carried out for steam to ethanol molar ratio equal to 9:1, for which the properties are given in Table 1. Generally, in order to improve the conversion efficiency, the reforming mixture is preheated in an evaporator before being fed to the reformer. From the literature, based on the temperature range over which various catalysts show good activity, 600°C was chosen as the inlet temperature for the preheated mixture. The flue gas temperature after combustion was obtained as the adiabatic flame temperature of ethanol combustion. These calculations pertain to a reformer design which can provide hydrogen to operate a

1kW PEM fuel cell, with a total of twenty one channels (i.e. ten reformer channels and eleven flue gas channels).

Table 1. Input conditions for Reformer and Flue gas channels

<i>Input parameter</i>	<i>Reforming channel</i>	<i>Combustor/ Flue gas channel</i>
Mass flow rate (kg/s)	2.4933×10^{-4}	5.5168×10^{-6}
Inlet Temperature (K)	873.15	2629.61
Mass fraction of ethanol at inlet	0.2211	-
Mass fraction of water vapor at inlet	0.7788	0.1843
Mass fraction of CO ₂ at inlet	-	0.1229
Mass fraction of N ₂ at inlet	-	0.6929

For both the reforming and combustor channels, prescribed mass flow rate at the inlet and atmospheric pressure condition at the outlet were specified. No slip condition was incorporated on all the walls of the plate type reformer, with conjugate heat transfer between channels. Steady laminar flow was considered. The first thirty thousand iterations were run using first order upwind scheme and for the rest of the iterations till convergence, second order upwind scheme was invoked. The kinetic parameters for the reforming reaction such as pre-exponential factor, stoichiometric coefficients, activation energy and order of the reaction were defined with respect to the individual species, specific catalyst and the corresponding reactions. In this case, the kinetic data corresponding to a single step reforming reaction over Pt-Ni catalyst was adopted from [19]. This reaction was taken as a surface reaction and was defined on the wall of the reforming channel. A density based solver was adopted for solving the flow and heat transfer equations. The material properties for the individual gases were defined using the ideal gas law for density, piece-wise polynomials for specific heat, kinetic theory based evaluations for viscosity and thermal conductivity. For the gaseous mixture, ideal gas law was used to calculate the density, ideal gas mixing law for specific heat, viscosity and thermal conductivity and kinetic theory for mass diffusivity.

The reforming fluid properties were computed based on the considerations listed in Table 2. For local convergence, all the flow variables were computed for residual error less than 10^{-6} . In addition, for ensuring convergence for the overall solution, the global mass imbalance between the inlet and outlet boundaries was ensured to be less than or equal to 1%.

2.2.2 Governing equations

The conservation equations of mass, momentum, energy and species were solved using Fluent 6.3 [20]. A single step global chemical reaction was considered for ethanol reforming, as follows:



Rate expression of the above equation [19] is

$$r_{\text{ethanol}} = k_r (\bar{c}_{\text{ethanol}})^\alpha (\bar{c}_{\text{water}})^\beta \quad (2)$$

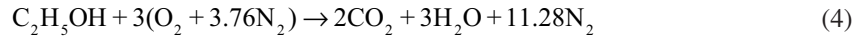
where,

$$k_r = k_o \exp\left(-\frac{\Delta E}{RT}\right) \quad (3)$$

$$\alpha = 1.01, \beta = -0.09, \Delta E = 59.3 \text{ kJ/mol}, k_o = 9.23 \text{ mol/gcat-h-atm}$$

The catalyst considered in the study is 0.3 wt%Pt-15 wt%Ni/ δ -Al₂O₃. For this catalyst, the density of the catalyst material can be calculated as 4746.2 kg/m³ and taking this into account, the pre-exponential factor k_o can be evaluated as equal to 487.53 (kmol/m³)^{0.08} s⁻¹.

Ethanol combustion is governed by the equation [20]



where,

$$-r_{\text{ethanol}} = k_r (\bar{c}_{\text{ethanol}})^\alpha (\bar{c}_{\text{oxygen}})^\beta \quad (5)$$

and k_r is of the form given in equation (3). Also, $\alpha = 0.15$, $\beta = 1.6$, $\Delta E = 125.6 \text{ kJ/mol}$ and $k_o = 8435 \times 10^6 \text{ kmol/m}^3\text{-s}$.

The rate expressions given above are used as source terms in the partial differential equations governing species transport. The governing equations for the reforming mixture are:

Continuity:

$$\frac{\partial \rho}{\partial t} + \nabla \cdot (\rho \vec{u}) = 0 \quad (6)$$

Momentum conservation:

$$\frac{\partial}{\partial t}(\rho \vec{u}) + \nabla \cdot (\rho \vec{u} \vec{u}) = -\nabla p + \nabla \cdot \bar{\tau} + \rho \vec{g} \quad (7)$$

where,

$$\bar{\tau} = \mu \left[\left(\nabla \cdot \vec{u} + \nabla \cdot \vec{u}^T \right) - \frac{2}{3} \nabla \cdot \vec{u} \mathbf{I} \right] \quad (8)$$

Species conservation:

$$\frac{d}{dx}(\dot{m}'' Y_i) - \frac{d}{dx} \left(\rho D \frac{dY_i}{dx} \right) = \dot{m}_i'' \quad (9)$$

Energy conservation:

$$\frac{\partial}{\partial t}(\rho E) + \nabla \cdot [\vec{u}(\rho E + p)] = \nabla \cdot \left[k_{\text{eff}} \nabla T - \sum_i h_i \vec{J}_i + (\bar{\tau}_{\text{eff}} \cdot \vec{u}) \right] \quad (10)$$

where,

$$E = h - \frac{p}{\rho} + \frac{\vec{u} \cdot \vec{u}}{2} \quad (11)$$

Ideal gas law for the gas mixture gives

$$p = \frac{\rho \bar{R} T}{M} \quad (12)$$

2.2.3 Grid selection

A uniformly-spaced structured mesh was generated throughout the domain with nodal spacing ranging from 0.125 – 1 mm. The grid independence test (Figs. 2 and 3) was performed for all the systems that were studied and a grid size of 0.25 mm was chosen for the subsequent studies after verifying insensitivity of the predicted results to further mesh refinement. For two-channel system, the grid independence study was done with counter-flow configuration, with aluminium as plate material. For the symmetric channel system considered later, the grid independent study was carried out using the co-flow configuration and the plate material was stainless steel. The predicted variations of reformer wall temperature and heat flux across the reformer wall were compared for different meshes. Here, the mesh with 1mm spacing corresponds to 400 cells, 0.5mm corresponds to 1600 cells, 0.25mm corresponds to 6400 cells and 0.125mm spacing corresponds to 25600 cells, respectively. Based on these simulations, a grid of 6400 cells was identified as optimum, for obtaining results of desired accuracy with moderate computational effort.

The flow inside the micro-channel pertains to low Reynolds number regime. As a result, boundary layers with steep spatial gradients are observed only close to the inlet and further downstream, the boundary layers from opposite walls merge to form fully developed flow. Since, the fully developed velocity and temperature profiles for laminar flow are polynomials of second and fourth order respectively, even a mesh with about eight nodes in the lateral direction is seen to be adequate.

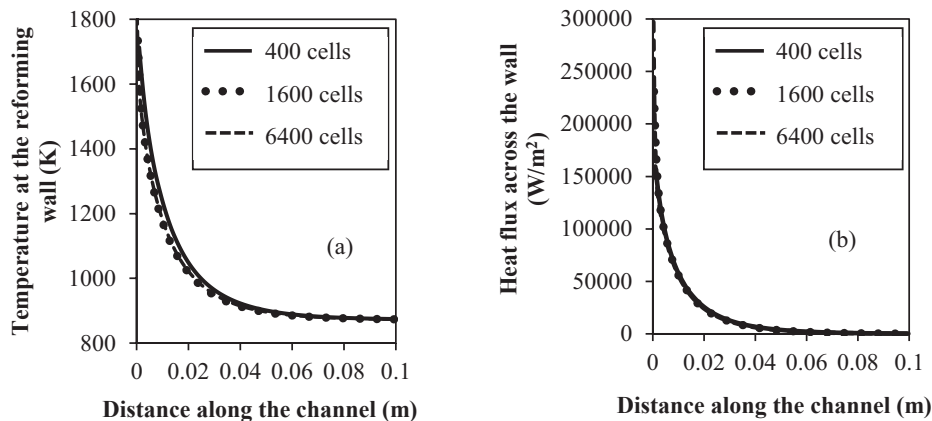


Figure 2. Grid independence study for two channel system using parameters such as (a) wall temperature (b) heat flux

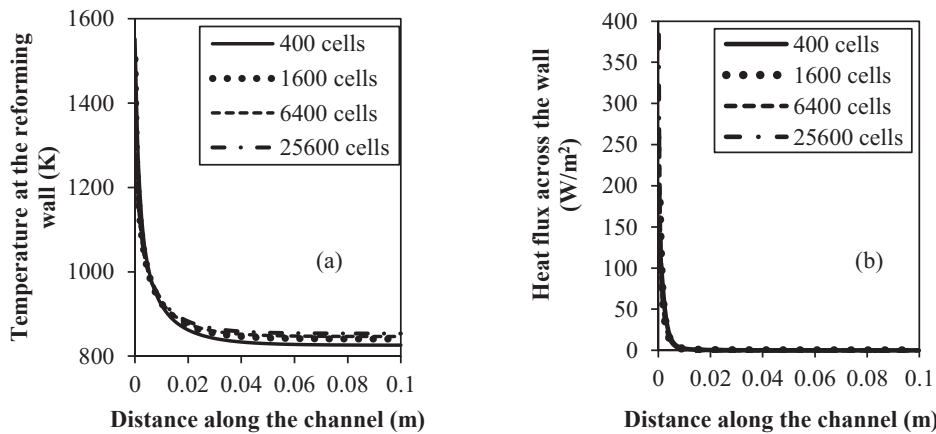


Figure 3. Grid independence study for symmetric channel system using parameters such as (a) wall temperature (b) heat flux

2.2.4 Validation of numerical results

The numerical methodology used in the present work was validated with the experimental work reported by Fatma et al. [19]. Figure 4 shows the comparison between the experimental results of [19] and those predicted by the present numerical model. It is observed that the present model is able to predict the results for ethanol conversion reasonably well at different mixture temperatures. The chemical kinetic parameters taken from the study of Fatma et al. [19] do not consider the effects due to the formation of methane. On the other hand, in the experimental work carried out by the authors, some methanation was observed which may affect the ethanol conversion. This could be the reason for the minor deviation seen in the predicted results of present work, from those of Fatma et al. [19].

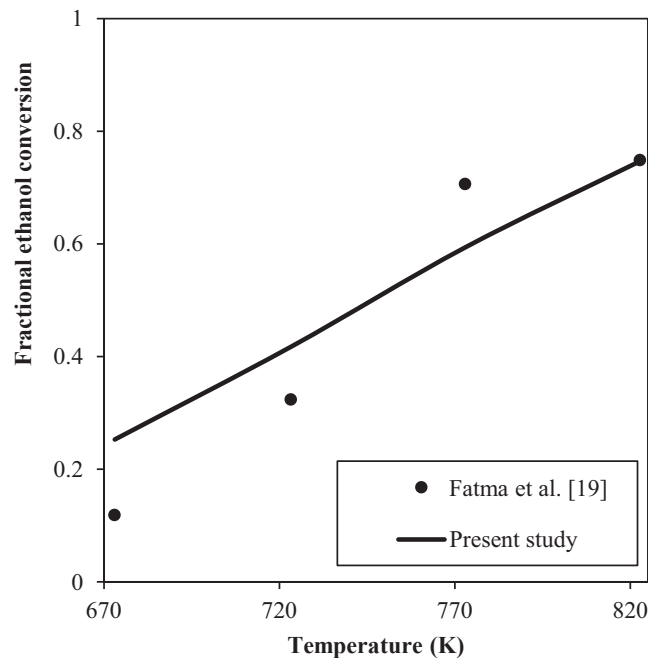


Figure 4. Effect of temperature on ethanol conversion

3. RESULTS & DISCUSSION

One of the important findings of the present study pertains to ethanol combustion in the reformer. The initial numerical study of reforming reaction in one channel and combustion in the other channel showed that even with highly refined meshes in the entry section, combustion is completed at a short distance from the inlet (Fig. 5). This is because the flame speed of ethanol is much greater than the average velocity of ethanol mixture. Furthermore, it is also difficult to sustain stable combustion in channels of small width, due to the quenching phenomenon. Hence, it is preferable that the combustion reaction takes place outside the reformer system to avoid combustion instabilities. Therefore, for further studies, flue gas obtained from combustion outside the reformer was used to provide the heat needed for the reforming reactions. From figure 5, it can be seen that while the combustion reaction is very fast and requires small length for completion, the reforming reaction is slow and requires longer length of the channel for its completion with heat transfer across the wall. This implies that the reforming reaction is dependent on the length across which the heat transfer takes place, due to its endothermic nature.

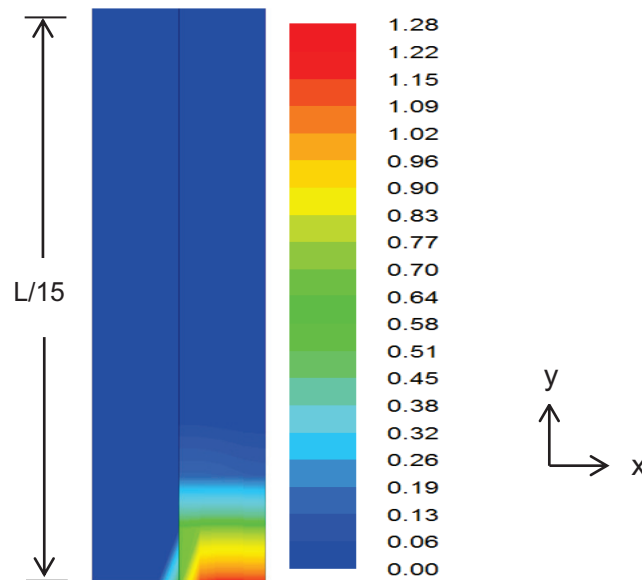


Figure 5. Reaction rate contour ($\times 10^{-4}$ kg mol/m³-s) of combustion in channel (magnified at the inlet)

A study comparing the performance of co-flow and counter-flow configurations with regard to reforming was done in the two-channel system. It is well known that for heat transfer, counter-flow is a more effective solution, in general; but for reforming reaction the results are observed to be better for co-flow (or) parallel flow arrangement as seen from Fig. 6. This is because, in the parallel flow configuration, the inlets of the reforming fluid and the flue gas channels are on the same side. As a result, near the inlet, the heat transfer through the channel wall is very high, which is desirable for initiating the endothermic (reforming) reaction. This is also evident from the high reaction rates of ethanol conversion observed near the inlet.

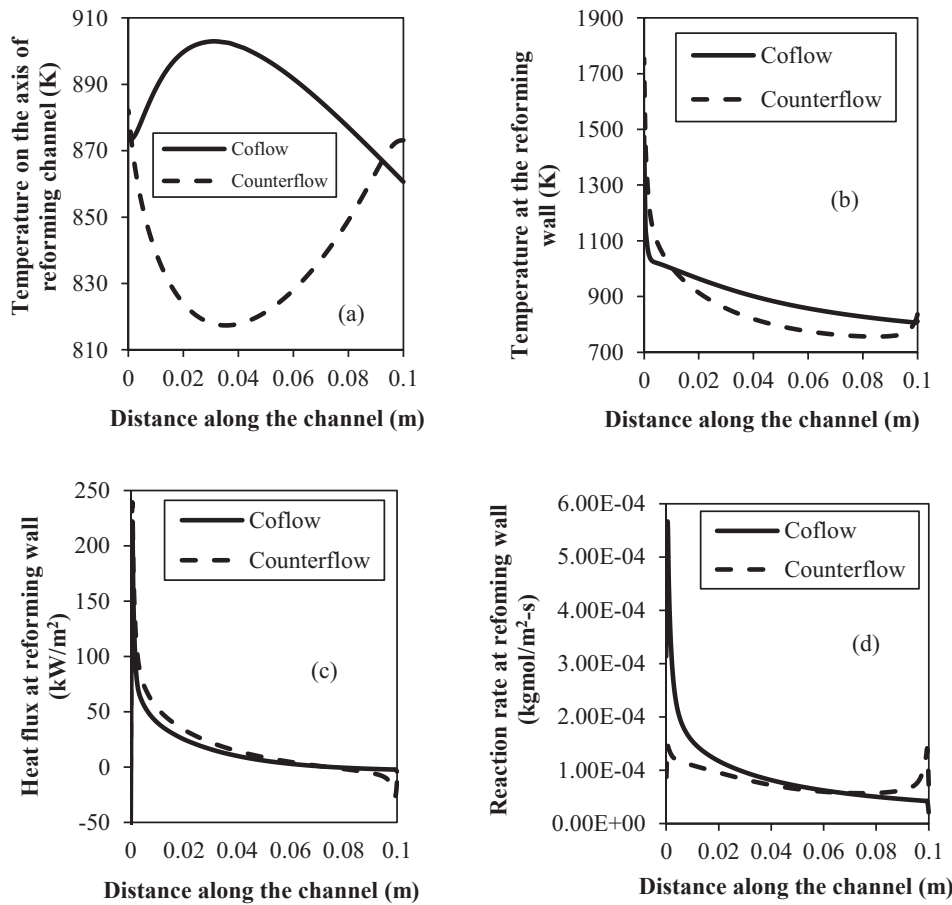


Figure 6. Two channel system: (a) Temperature across the center of the reformer channel (b) Wall temperature distribution (c) Heat flux distribution (d) Reaction rate distribution

In the 2-channel system, only one wall of the reformer gets involved in the heat transfer and reforming reaction. Hence, the next study was done with a 3 channel system as shown below. This was to understand the effectiveness of heat transfer from both the side walls of the reforming channel. Here again the comparative study of co-flow and counter-flow was carried out and it is seen that the co-flow configuration is better for reforming, as shown in the plots of figure 7.

Since the conversion rate depends upon the amount of heat transferred to the reforming mixture undergoing endothermic reaction, it is evident that supplying heat from both sides is helpful. The conversion rate therefore increases for the three channel system, as compared to the two channel system. Thus, it is proposed that in a multi-channel system the two end channels should be flue gas channels so that there is continuity in the arrangement of double-side heating for all the reformer channels. Since the co-flow configuration has been shown to provide better results for SRE, only co-flow situation has been studied further.

In order to understand the performance of the system with increase in the number of channels, eleven channel systems were studied. The eleven channel system considered for the study is arranged such that the second, fourth, sixth, eighth and the tenth channels carry the reforming fluid and the rest of the channels correspond to flue gas. In figure 9, the length has been zoomed in between 0 – 10mm in order to visualize and understand the variation of temperature in different channels. Due to symmetry, results for the first six channels only are shown. The centre line temperatures of the three flue gas channels and three reformer channels indicate that the end effects are limited to only the outer-most flue

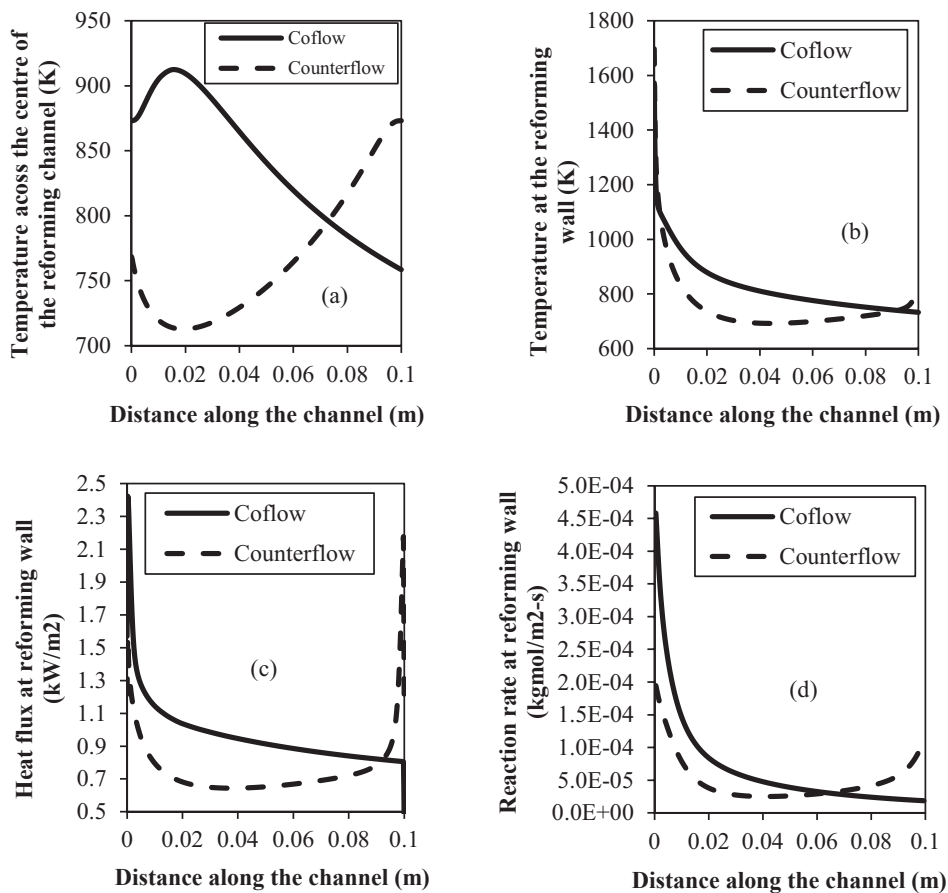


Figure 7. Three channel system: (a) Temperature across the center of the reformer channel (b) Wall temperature distribution (c) Heat flux distribution (d) Reaction rate distribution

gas and reformer channels. All the interior flue gas channels have essentially the same temperature variation. Similarly, all the interior reformer channels have the same temperature variation with axial distance. It is also evident that in the co-flow arrangement, most of the heat transfer occurs in the initial 10% of the channel length and a significant fraction of the ethanol reforming reaction occurs within this zone. Furthermore, the temperature differences are less than approximately 10K beyond this initial length. Parallel temperature curves for the different channels at larger axial distances implies good conjugate heat transfer across the walls, similar to the observations made by various authors [21 - 24] earlier. It is also clear that the symmetric (half combustor + reformer + half combustor) model is a good representation of a large multi-channel reformer system, since all the interior reformer and flue gas channels have identical velocity and concentration profiles.

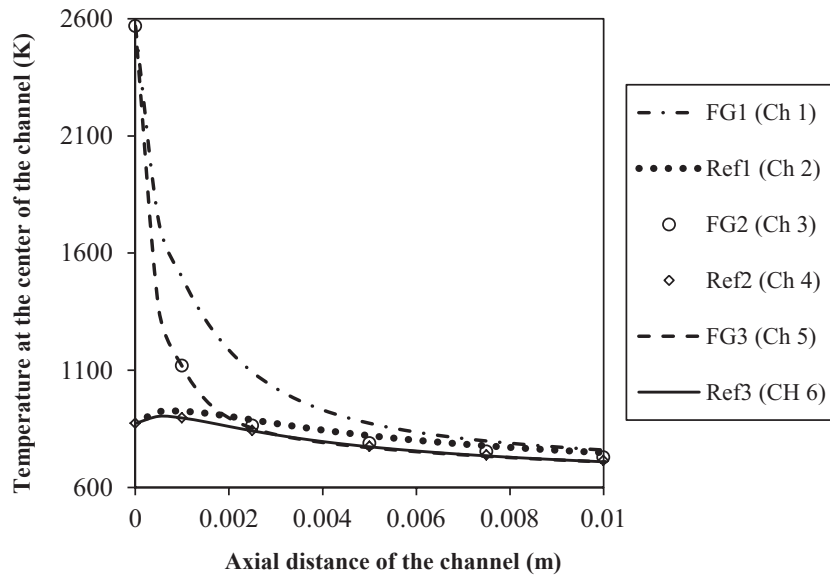


Figure 9. Temperature distribution for eleven channel system at the center of the channel

The results predicted for a symmetric channel system are shown in Figs. 10a – f. The axial temperature profile within the reformer exhibits an initial spike from 873K to about 1400K at the wall and a milder spike in temperature at the axis. For larger axial distances, the temperature values at the wall and axis are close to each other and they decrease in a similar manner. This is in confirmation with the heat transfer characteristics of co-flow configuration and the endothermic reforming process which consumes heat. Fig. 10(b) shows that the variation of pressure within the channel is negligible (of the order of few Pascals) and hence the situation may be treated essentially as a constant pressure chemical reaction. In Fig. 10(c) the slight increase seen in the ethanol mass fraction after the initial depletion is due to diffusion of ethanol from interior parts of the reformer channel. When ethanol at the wall is consumed close to the inlet due to high reaction rate, strong species gradients are created near the wall in the lateral direction and hence, ethanol from the center of the channel diffuses towards the wall. As a result, the ethanol concentration at the wall increases with axial distance initially. Later, the global concentration of ethanol decreases inside the channel due to consumption by the reforming reaction. These phenomena can explain the trends in the variation of concentration plots of H_2O , CO_2 and H_2 as well. Lighter species such as hydrogen and water vapor do not exhibit much variation in the lateral direction (between the wall and the axis) due to their higher mass diffusivities. On the other hand, heavier species like ethanol and carbon dioxide exhibit some differences between the concentrations at the wall and the axis.

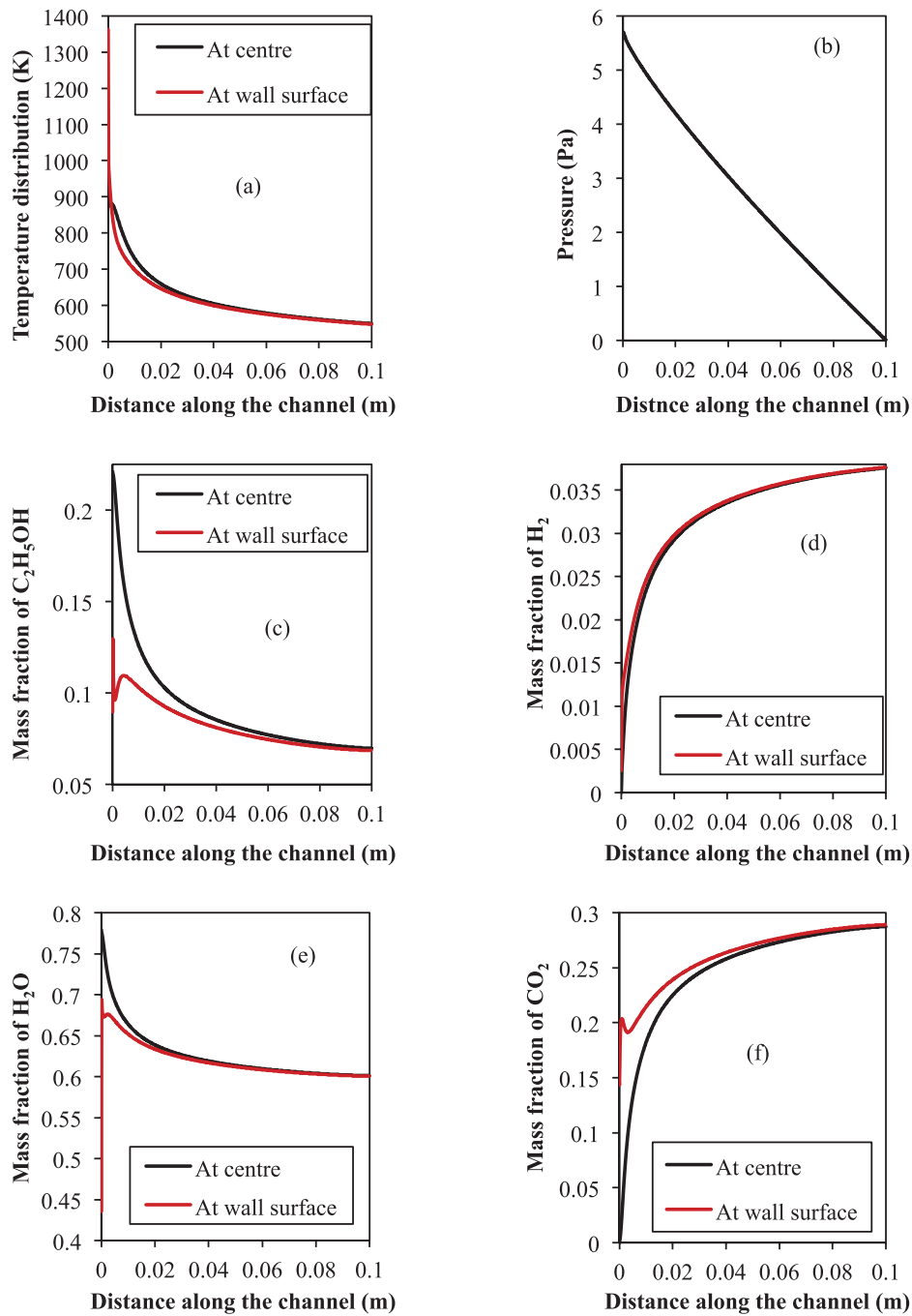


Figure 10. Symmetric channel system, distributions of - (a) Temperature (b) Pressure (c) Ethanol mass fraction (d) Hydrogen mass fraction (e) Water vapor mass fraction (f) Carbon dioxide mass fraction, along the reformer

Figures 11 (a) and (b) depict the hydrodynamic and thermal development of the flow in the symmetric channel system. The flow seems to be developing throughout the length of the channel. The velocity profile (Fig. 11a) develops into the parabolic shape corresponding to fully developed flow within a short axial distance. For larger axial distances, however, the velocity profiles exhibit a mild variation particularly in the maximum velocity value on the axis. This can be attributed to the influence of the reforming reaction, which causes an increase in the hydrogen concentration and decrease in temperature along the length of the channel thereby resulting in a change of gas density. The density change affects the velocity profile and hence the flow continues to develop throughout the channel length. Another interesting feature seen in the cross-stream variations of the temperature and concentration profiles is that the profiles become nearly flat, at larger axial distances. It is evident from these profiles that the reforming reaction is not diffusion-controlled in the rear portion of the channel. It is primarily influenced by the heat transfer across the wall, which in turn, affects the wall temperature variations. The kinetics of the reforming reaction depends upon the wall temperature.

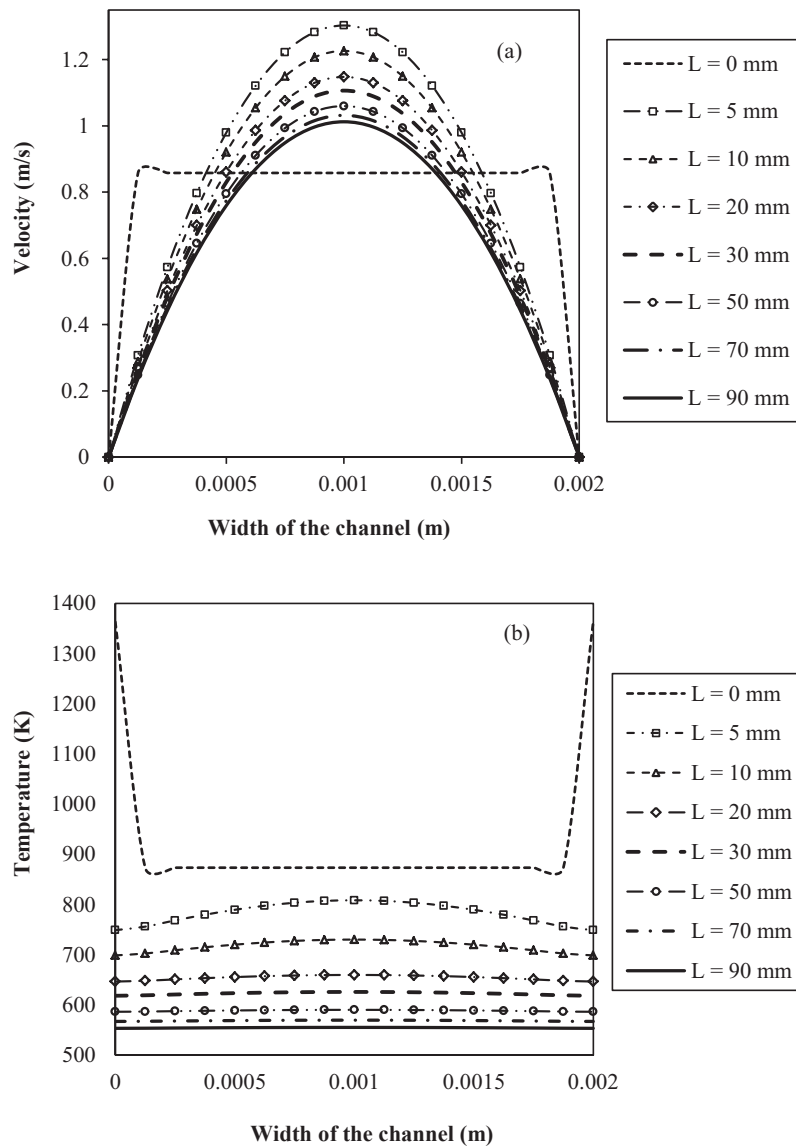


Figure 11 continued

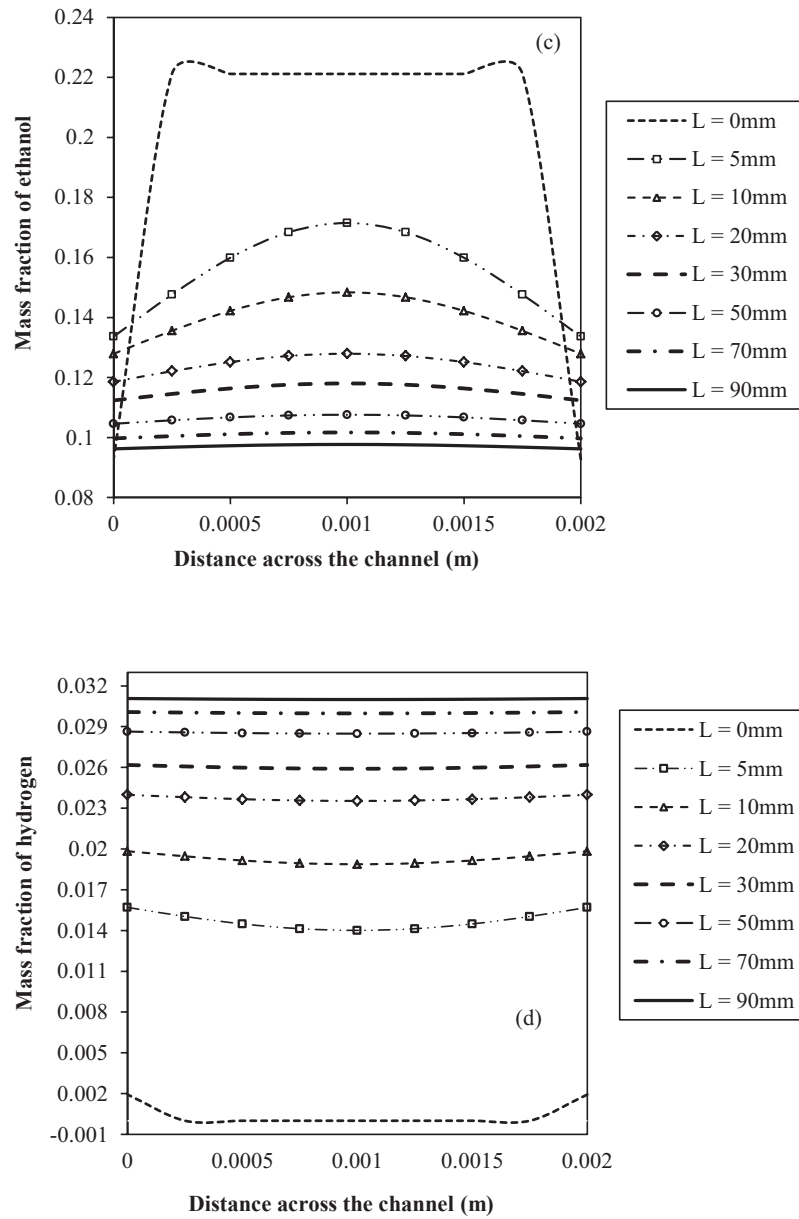


Figure 11. (a) Velocity profile (b) Temperature profile (c) Ethanol mass fraction profile (d) Hydrogen mass fraction profile, across the channel width

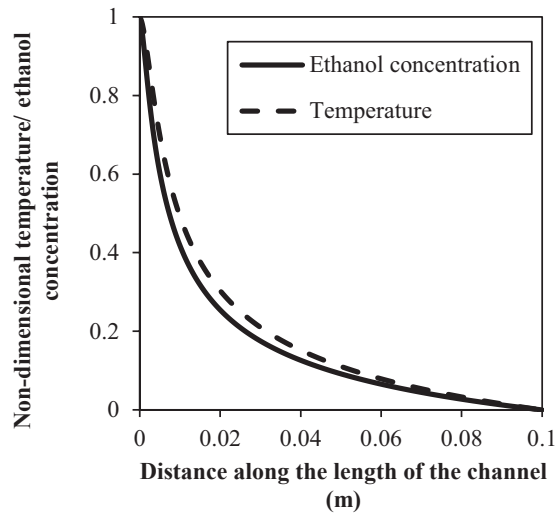


Figure 12. Behavior of normalized parameter along the length of the channel

In order to understand the parameters controlling the reaction, the temperature and ethanol concentration were normalized with respect to their inlet and outlet values, as shown in Fig. 12. It is seen that the two normalized parameters follow a similar trend. This provides an additional corroboration for the suggestion that the endothermic reforming reaction is controlled mainly by the conjugate heat transfer across the wall.

Studies were done with systematic variations in the geometric parameters in order to understand their influence on ethanol consumption and hydrogen production. As discussed earlier, the length of the channel does not affect beyond a certain value. Hence, co-flow configurations with shorter lengths are desired, in general. It is also seen that when the width of the channel is increased, the effective heat transfer increases due to increase in area, thus leading to increase in ethanol conversion.

A one-dimensional heat transfer analysis between the combustor and the reformer channels can bring to light the effects of some of the geometrical parameters. For instance, the overall heat transfer coefficient (U) between the flue gas and the reformer gas streams can be evaluated as:

$$\frac{1}{U} = \frac{1}{h_r} + \frac{t_w}{k_s} + \frac{1}{h_f} \quad (13)$$

where h_r and h_f are the heat transfer coefficients for the reformer and flue gas sides, t_w is the wall thickness and k_s is the thermal conductivity of the wall material. For fully developed flow, the heat transfer coefficients themselves can be expressed in the form of:

$$h = c \cdot \frac{k_g}{\left(\frac{t}{2}\right)} \quad (14)$$

where t is the channel gap and k_g is the thermal conductivity of the respective gas flow stream. In the above expression c is the fully developed flow Nusselt number which is a constant. The heat flux between the flue gas and the reformer stream is given as:

$$\frac{Q}{(2A_w)} = U(T_f - T_r) \quad (15)$$

where, T_f and T_r are the bulk temperatures of the flue gas and reformer gas, at the particular axial location. The wall area A_w can be evaluated as:

$$A_w = L \times W \quad (16)$$

where, L and W are the length and width of the channels.

Thus, it is evident that all the geometric parameters (L , W and t) affect the rate of conjugate heat transfer between the two gas streams and hence the conversion rate of ethanol. Since, shorter length is more effective for parallel flow configuration, for the same heat transfer area, it is advantageous to increase the width rather than the length. For a larger channel width, the convective film resistances become more dominant than the conduction resistance across the wall. This results in a larger wall temperature on reformer side at higher channel gap (t) values, which in turn, helps to achieve higher reaction rate for the reforming reaction, as shown in the schematic figure 13. Thus, a maximum conversion of 84% is obtained for the case with smaller length ($L = 50\text{mm}$), larger width ($W = 100\text{mm}$) and larger channel gap ($t = 2\text{mm}$) as shown in Table 2.

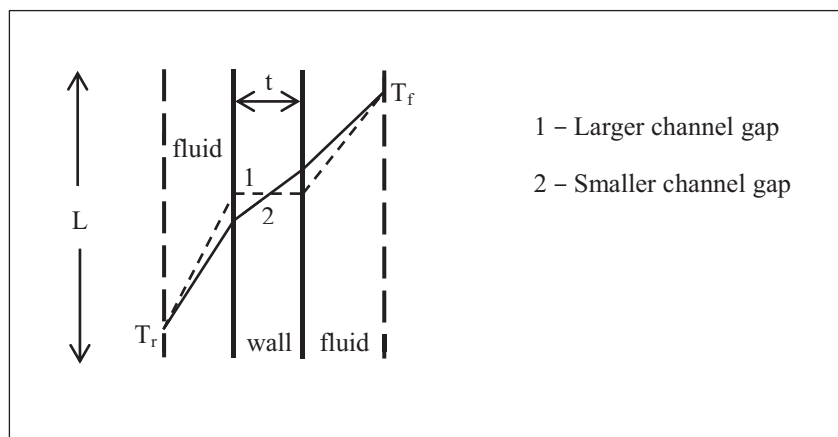


Figure 13. Temperature profile across the walls

Table 2. Comparison of ethanol conversion for different geometric configurations

Configuration (Length x width x depth) mm^3	Ethanol conversion %
50 x 50 x 1	59.27
50 x 50 x 2	78.39
50 x 100 x 1	82.77
50 x 100 x 2	84.28
100 x 50 x 1	64.47
100 x 50 x 2	54.32
100 x 100 x 1	69.85
100 x 100 x 2	68.48

A comparison of the time scales for kinetics, mass diffusion and flow (residence time) show that chemical kinetics and species diffusion are relatively faster ($t_{kin} \sim 10^{-5} \text{ s} < t_{diff} \sim 10^{-2} \text{ s} < t_{residence} \sim 10^{-1} \text{ s}$). Thus the ethanol conversion primarily depends on heat transfer across the channels, which provides the energy needed to complete the endothermic reaction.

It has to be noted here that in the present study, the reformer plates have no corrugations as a 2-D model is employed. With the incorporation of corrugations (or internal fins) on the plates, it is expected that the conversion rate would increase, due to increase in surface area. Furthermore, in the steady state simulation considered in the present work, the thermal capacity of the wall material does not play a role. At larger wall thickness values, the dynamics of reforming reactions could be influenced by thermal storage in the walls also.

5. CONCLUSIONS

This paper presents a numerical study of reforming in a micro-channel plate-type reactor with ethanol as fuel. Simulations were done on a 2-D domain for different channels, starting with simplified two-channel systems to a more practical system with multiple channels. Simulations show that it is better to complete combustion outside the micro-channel device and feed the flue gas into the reformer for providing the heat needed by the endothermic reforming reactions. While comparing the 2-channel and 3-channel systems, it is observed that for better efficiency, each reforming channel must have a flue gas channel for heating on either side. From the present studies, it is concluded that a parallel flow arrangement is optimal for obtaining higher ethanol conversion in multiple channel systems. This is because high heat transfer rate in the inlet region initiates the reforming reaction and contributes significantly to the overall conversion of ethanol. The profiles of velocity, temperature and species concentrations attain fully developed profiles quickly, at short axial distance from the inlet. However, further slow variations do occur with axial length due to changes in gas density and the consumption of ethanol in the reforming reaction. The temperature and concentration profiles essentially become flat indicating the weak effect of diffusion on reforming. The rate controlling mechanism appears to be the conjugate heat transfer across the flue gas and reformer channels. Conjugate heat transfer, in turn, is influenced by the convection film resistances on the flue gas and reforming mixture sides, as well as the heat transfer area. The studies show that maximum conversion efficiency can be obtained for relatively smaller length, larger width and larger channel gap, for the co-flow configuration.

NOMENCLATURE

D	Diffusion coefficient (m^2/s)
ΔE	Activation energy of a reaction (J/kg)
Ch	Channel
E	Energy (J)
FG	Flue gas
I	Unit tensor
J	Diffusion flux (s^{-1})
\bar{M}	Molecular weight (kg/kmol)
\bar{R}	Universal gas constant ($\text{J}/\text{kmol}\cdot\text{K}$)
Ref	Reformer
SRE	Steam reforming of ethanol
S_h	Source term for heat (J)
T	Temperature (K)
Y	Mass fraction
\bar{c}	Molar concentration (kmol/m^3)
g	Acceleration due to gravity (m/s^2)
h	Enthalpy (J/kg)
\dot{m}''	Mass flux ($\text{kg}/\text{m}^2\cdot\text{s}$)
\dot{m}'''	Mass production rate per unit volume ($\text{kg}/\text{m}^3\cdot\text{s}$)

k_o	Pre-exponential factor
k_r	Reaction rate constant (kg/mol-s)
p	Pressure (Pa)
r	Specific rate of reaction (mol/kg-s)
t	Time (s)
u	Velocity (m/s)

Greek symbols

α, β	Reaction order
ρ	Density (kg/m ³)
μ	Dynamic viscosity (Pa-s)
τ	Shear stress (Pa)

Subscripts

i	Species i
eff	Effective

Superscript

=	Tensor notation
→	Vector notation

ACKNOWLEDGEMENTS

The authors wish to thank the Centre for Fire, Explosive & Environment Safety (CFEES), Defense Research and Development Organization (DRDO), India, for providing the financial support necessary for this study.

REFERENCES

- [1] Wanat E. C., Venkataraman K., Schmidt L. D., "Steam reforming and water-gas shift of ethanol on Rh and Rh-Ce catalysts in a catalytic wall reactor", *Applied Catalysis A: General*, 276 (1-2), pp. 155-162, (2004).
- [2] Sahoo D. R., Vajpai S., Patel S., Pant K. K., "Kinetic modeling of steam reforming of ethanol for the production of hydrogen over Co/Al₂O₃ catalyst", *Chemical Engineering Journal*, 125 (3), pp. 139-147, (2007).
- [3] Leclerc S., Mann R. F., Peppley B. A., The CANMET Energy Technology Centre (CETC), "Evaluation of the catalytic ethanol-steam reforming process as a source of hydrogen-rich gas for fuel cells", Le Centre, Ressources naturelles Canada, 1998.
- [4] Vaidya P.D., Rodrigues A.E., "Insight into steam reforming of ethanol to produce hydrogen for fuel cells", *Chemical Engineering Journal*, 117 (1), Issue 1, pp. 39-49, (2006).
- [5] Suna J., Qiu X-P., Wu F., Zhu W-T., "H₂ from steam reforming of ethanol at low temperature over Ni/Y₂O₃, Ni/La₂O₃ and Ni/Al₂O₃ catalysts for fuel-cell application", *International Journal of Hydrogen Energy*, 30 (4), 437-445, (2005).
- [6] Simson A., Waterman E., Farrauto R., Castaldi M., "Kinetic and process study for ethanol reforming using a Rh/Pt washcoated monolith catalyst", *Applied Catalysis B: Environmental*, 89 (1-2), pp. 58-64, (2009).
- [7] Aboudheir A., Akandea A., Idema R., Dalai A., "Experimental studies and comprehensive reactor modeling of hydrogen production by the catalytic reforming of crude ethanol in a packed bed tubular reactor over a Ni/Al₂O₃ catalyst", *International Journal of Hydrogen Energy*, 31 (6), pp. 752-761, (2006).
- [8] Peela N. R., Mubayi A., Kunzru D., "Steam reforming of ethanol over Rh/CeO₂/Al₂O₃ catalysts in a microchannel reactor", *Chemical Engineering Journal*, 167 (2-3), pp. 578-587, (2011).

- [9] Karakaya M., Avci A., "Simulation of On-Board Fuel Conversion in Catalytic Microchannel Reactor-Heat Exchanger Systems", *Topics in Catalysis*, 52 (13-30), pp. 2112–2116, (2009).
- [10] Casanovas A., Domínguez M., Ledesma C., López E., Llorca J., "Catalytic walls and micro-devices for generating hydrogen by low temperature steam reforming of ethanol", *Catalysis Today*, 143 (1-2), pp. 32–37, (2009).
- [11] Casanovas A., de Leitenburg C., Trovarelli A., Llorca J., "Catalytic monoliths for ethanol steam reforming", *Catalysis Today*, 138 (3-4), pp. 187–192, (2008).
- [12] Casanovas A., Saint-Gerons M., Griffon F., Llorca J., "Autothermal generation of hydrogen from ethanol in a microreactor", *Int. J. Hydrogen Energy*, 33 (7), pp. 1827–1833, (2008).
- [13] Llorca J., Casanovas A., Trifonov T., Rodríguez A., Alcubilla R., "First use of macroporous silicon loaded with catalyst film for a chemical reaction: amicroreformer for producing hydrogen from ethanol steam reforming", *Journal of Catalysis*, 255 (2), pp. 228–233, (2008).
- [14] Wang J., Liu G., Xiong Y., Huang X., Guo Y., Tian Y., "Fabrication of ceramic microcomponents and microreactor for the steam reforming of ethanol", *Microsystem Technologies*, 14 (9-11), pp. 1245–1249, (2008).
- [15] Lim M. S., Kim M. R., Noh J., Woo S., "A plate-type reactor coated with zirconia-sol and catalyst mixture for methanol steam-reforming", *Journal of Power Sources*, 140 (1), pp. 66–71, (2005).
- [16] Liubov K-M., Renken A., "Microstructured reactors for catalytic reactions", *Catalysis Today*, 110 (1-2), pp. 2-14, (2005).
- [17] Cominos V., Hessel V., Hofmann C., Kolb G., Zapf R., Ziogas A., Delsman E. R., Schouten J. C., "Selective oxidation of carbon monoxide in a hydrogen-rich fuel cell feed using a catalyst coated microstructured reactor", *Catalysis Today*, 110 (1-2), pp. 140-153, (2005).
- [18] Kolb G., Zapf R., Hessel V., Lowe H., "Propane steam reforming in micro-channels – results from catalyst screening and optimisation", *Applied Catalysis A: General*, 277 (1-2), pp. 155-166, (2004).
- [19] Fatma S-B., Erhan A. A., Ilsen O. Z., "Steam reforming of ethanol over Pt–Ni Catalysts", *Catalysis Today*, 138 (3–4), pp. 183-186, (2008).
- [20] *Fluent User Guide*, Fluent 6.3.26, from <http://www.fluent.com>, (2005).
- [21] Zanfiri M., Gavriilidis A., "Catalytic combustion assisted methane steam reforming in a catalytic plate reactor", *Chemical Engineering Science*, 58 (17), pp. 3947-3960, (2003).
- [22] Zanfiri M., Gavriilidis A., "Influence of Flow Arrangement in Catalytic Plate Reactors for Methane Steam Reforming", *Chemical Engineering Research and Design*, 82 (2), pp. 252-258, (2004).
- [23] Petrachi G. A., Negro G., Specchia S., Saracco G., Maffettone P. L., Specchia V., "Combining Catalytic Combustion and Steam Reforming in a Novel Multifunctional Reactor for On-Board Hydrogen Production from Middle Distillates", *Industrial & Engineering Chemistry Research*, 44 (25), pp. 9422–9430, (2005).
- [24] Peela N. R., Kunzru D., "Steam Reforming of Ethanol in a Microchannel Reactor: Kinetic Study and Reactor Simulation", *Industrial & Engineering Chemistry Research*, 50 (23), pp. 12881–12894, (2011).